OPTICAL METHODS FOR IN-PROCESS MONITORING OF LASER BEAM WELDING

Fredrik Sikström[1], Morgan Nilsen[1], Ingemar Eriksson[2]

[1]Department of Engineering Science, University West, Trollhättan, Sweden
[2]GKN Aerospace, Trollhättan, Sweden

fredrik.sikstrom@hv.se

This paper addresses the issue of evaluating and selecting optical sensors to be integrated with a 1µm laser beam welding system. The method used for this evaluation is mainly a survey of relevant research litterature. The result of this work is a matrix showing the different methods and distinct features related to relevant process conditions that can be estimated or detected with respective methods. This evaluation also includes considerations on the required sensor bandwidth in relation to inertia and time constants in the physical process.

Keywords: Optical Methods, Process Monitoring, Laser Beam Welding

1. INTRODUCTION

Automation of laser beam welding (LBW) by means of in-process monitoring and control has been addressed by many researchers see e.g. (Regaard, Kaierle et al. 2009; Huang and Kovacevic 2011; Schmitt, Mallmann et al. 2012; Sibillano, Rizzi et al. 2012; Chen, Zhang et al. 2013). Different novel approaches have been suggested and tested, but industrial implementation of research results is so far limited. The reasons are most likely the harsh nature of LBW processes due to excessive heat flux, possibly high intensity laser scattering, and evaporations of material etc. Another reason for the limited use of in-process sensors is the industrial need of mechanical robustness and flexibility in welding tools, and external devices can impose restrictions on how the system can be used in real production.

In order to make in-process monitoring feasible in future industrial welding automation, research needs to be focused on the following directions: seamless integration of the sensor in the processing head to allow its operation with complex work pieces with difficult access; fast and robust detection and monitoring capabilities; and development of sensor fusion strategies. The proposed measures will permit in-process monitoring and real-time detection of process defects and thereby facilitate for improved quality by detection and possible automatic adaption of process parameters.

One approach to handle these questions is to use optical sensors. The possibility to non-intrusive measurements from a distance make them less sensitive to the hostile environment. There might also be a possibility to mount the sensor coaxial in the same beam path as the processing laser beam, making the installation robust and compact. Depending on the optical emissions to be observed and the required bandwidth, different sensor types, different spectral ranges, different fields of view and different sensor positions can be applied.

Typical geometrical processing problems under consideration here are joint gap variations, uncertainty in seam position, base metal thickness variation, focal point position, and misalignment. Typical intrinsically physical process problems are pore and spatter formations together with lack of fusion and lack of penetration. The last two problems are considered as the most severe problems and robust monitoring and detection of these is a major aim.

This paper addresses the issue of evaluating and selecting optical sensors to be integrated with a 1µm LBW system. The method used for this evaluation is mainly a survey of relevant research litterature. The result of this work is a matrix showing the different methods and distinct features related to relevant process conditions that can be estimated or detected with respective methods. This evaluation also includes considerations on the required sensor bandwidth in relation to inertia and time constants in the physical process. In order to understand the applicability of the different methods an experimental estimation of the optical transmission of a typical LBW tool has been carried out. This information gives together with information of typical process emissions insight on the physical constraints for the different monitoring methods.

1.1. Sensors integrated in a LBW tool

A typical LBW processing tool augmented with integrated sensors is shown in Fig. 1. This basic tool consists of an optical system for laser beam focusing including a collimating lens, a 45° dichroic mirror and a focusing lens. The laser power source also supplies a visible low power pilot beam (typically at 650 nm) to be used during the setup of a laser welding session. In addition the tool is equipped with optical sensors (or sensor inlets) all arranged coaxial to the laser processing beam through optics and semi-transparent mirrors.

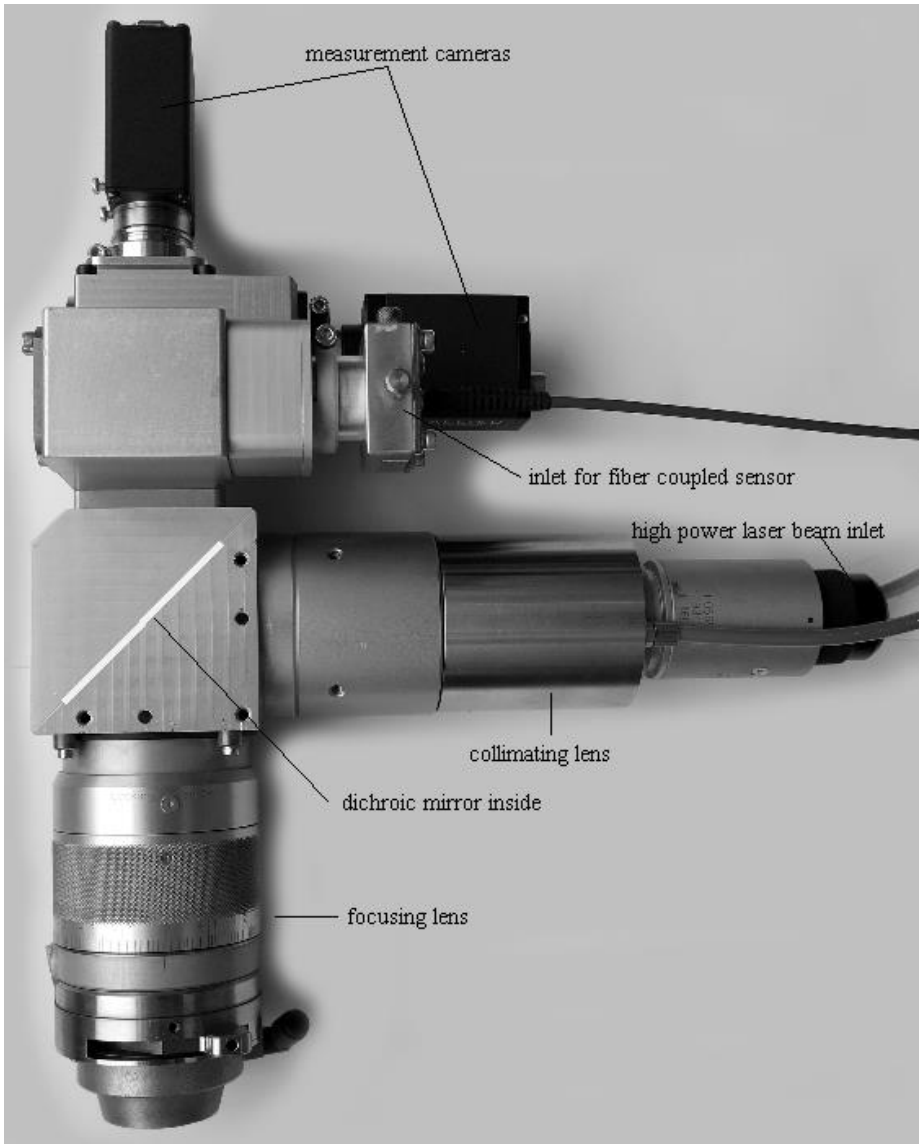

Fig. 1. A LBW optical head equipped with inline sensors.

1.2. The 1µm laser beam welding process

The welding process considered is high-power 1µm keyhole LBW, enabling deep penetration at high processing speeds and high aspect-ratio welds (depth/width). When the power density of the laser beam typically is above

1MW/cm^2, the molten metal in the beam focus starts to evaporate. The recoil pressure of the vapour pushes the melt aside, creating a capillary filled with hot metal gas. This capillary is known as the keyhole and can extend over the complete depth of the sheet metal. A radiant body, a plume, is formed above the weld pool containing vaporised material ejected from the keyhole. The plume is composed of very small particles, with an average diameter less than 50nm, and that the particles cluster together as they condense (Steen and Mazumder 2010). The temperature of the plume, is less than 3000K corresponding to the boiling point of relevant welding alloys (Greses, Hilton et al. 2004). Although the vapour plume probably is neither in thermal equilibrium with the surrounding nor a perfect black body, black-body radiation can be used as a first approximation for the energy they emit.
Several parameters restricted to a relative narrow parameter space are involved in the control of LBW. The most significant parameters are, laser power density, the position of the focal point, welding speed, filler material (feed rate and composition), shielding gas (flow rate and composition) gaps and seam geometry among other. Laser power density in the focal plane (controlled by the laser beam quality, the optics used) and welding speed gives the gross energy which have a major influence on the weld depth and width. Seam gap width, sheet metal thickness and welding speed determine the filler material rate. The position of the focal point influences weld penetration depth and geometry. The shielding gas also affect the penetration depth and determine the welding speed.

The LBW process is inherently characterised by a relative degree of instability, mainly due to variations in material properties and the complex interaction between mechanisms such as laser absorption, the metal evaporation, vapour pressure in the keyhole and melt flow. This instability can causes unwanted welding defects, such as porosities and variations in the penetration depth. The process dynamics of LBW also displays a time constants that are in the order of milliseconds. Table 1 gives some references to experimentally estimated LBW dynamics.

Table 1. Typical time constants of keyhole and weld pool dynamics.

Feature	Time scale
Weld pool width	20 ms (Beersiek 2001)
Keyhole formation	0.5-5ms (Fujinaga, Takenaka et al. 2000; Perret, Bizouard et al. 2001)
Keyhole width	5ms (Beersiek 2001)

2. RELEVANT OPTICAL METHODS

A number of relevant optical monitoring methods has been identified all with the common feature that they can be applied coaxially in the same beam path as the processing laser beam. The methods are cameras (visual and infrared, sometimes in combination with a projected laser line), spectral measurements (photodiodes and spectroscopy), confocal methods, white light interferometry and laser ultrasonic. Some of the methods have potential to be used for in-process monitoring whereas other has to be applied for pre- or post-process monitoring. Their respective sensor bandwidth is summarised in Table 2 for a comparison of their applicability to relevant welding features.

2.1. Vision and infrared cameras

Vision- and infrared cameras are sensitive in different ranges of spectral emissions and can therefore be tuned e.g. by optical band pass filters to suppress disturbances and enhance geometrical features in the process. With cameras coaxial to the optical path of the processing head is it possible to monitor e.g. the stability of the keyhole for spatter detection, the joint position for seam tracking, the width of the weld pool that during certain conditions are correlated to weld penetration (Jager and Hamprecht 2009; Heralic, Christiansson et al. 2010; Kim and Ahn 2012; M., M. et al. 2012).

Typically the LBW scene is covering a very broad range of illumination which must be obtained with a minimum loss of information. One would like to capture the geometrical features surrounding the melted welding area together with the very high intensity processing light. High dynamic range imaging (HDR >=120dB) is thus crucial when using visual cameras in the presence of processing emissions. It is essential to take full advantage of the quantification levels provided by the image sensor. It has been found that a Lin-Log CMOS sensor satisfies this demand by an adjustable intensity response curve that combines linear and

logarithmic responses (Bandoh, Guoping et al. 2010). See Fig. 2. for an example of inline images from a Lin-Log CMOS camera showing the influence of this plume to visual monitoring.

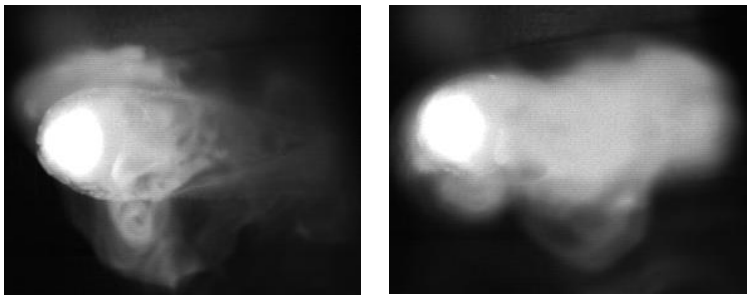

Fig. 2. Two conditions of the vapour plume captured with a visual camera. Left figure shows a course plume revealing the shape of the melted weld pool. Right figure shows a dense plume hiding the weld pool.

2.2. Laser profile sensors

Laser profile sensors are based on the principle of laser triangulation and have been proven useful in both seam-tracking applications (Regaard, Kaierle et al. 2009) and for weld geometry measurements (Huang and Kovacevic 2011). A typical laser profile sensor consists of a low power laser diode and a pattern generator to create a laser stripe and an image sensor (CCD or CMOS) with a focus lens and optical filter to capture the profile. When used with LBW the image sensor can be integrated into the welding head to reduce size and enable measurement coaxial to the power laser beam. Image sensor and laser diode is placed at an angle α between them as shown in Fig. 3, where α represents the angle between the optical axis of the lens and the laser beam.

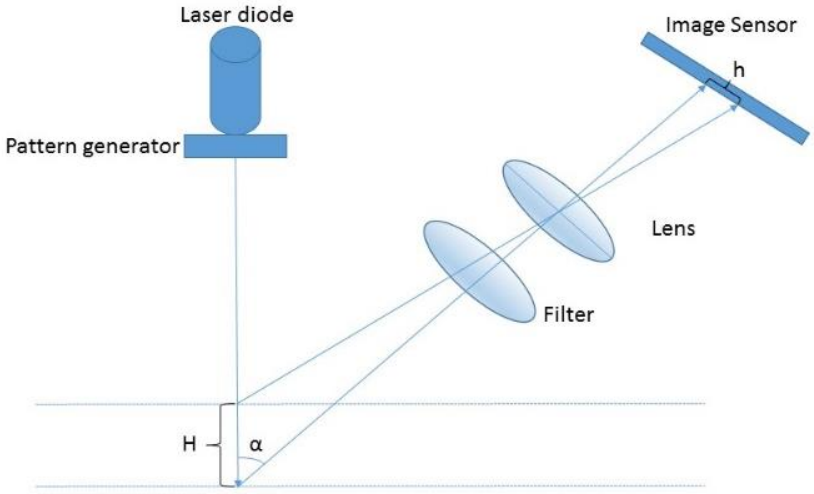

Fig. 3. Typical setup of a laser profile sensor.

Light from the laser diode is reflected back from the measurement object to the image sensor creating a profile representing the reflected laser stripe. Distance and lateral position between the sensor and the measurement object can be calculated based on the mathematical relationship of the geometrical optics in the setup. A change in distance (H) will cause a proportional change (h) on the image sensor. An image processing algorithm is then applied which extracts the laser stripe profile reflected on the image sensor and calculates the distance from the sensor and the measurement object for each pixel of the profile.

2.3. Photodiodes and spectroscopy

Photodiodes (Yousuke, Terumasa et al. 2009; Stritt, Weber et al. 2011) and spectrometers can be used to monitor optical process emissions such as reflections from the processing laser beam and thermal emissions from the vapour plume and keyhole. These emissions can be correlated to the stability of the process and detect features related to the status of the keyhole (Kong, Ma et al. 2012; Sibillano, Rizzi et al. 2012; Chen, Zhang et al. 2013).

2.4. Inline coherence imaging

Inline coherence imaging is based on spectral domain optical coherent tomography that is commonly used in biological applications (Webster, Wright et al. 2011). This method has the ability to measure key hole depths in real-time and can be used in LBW applications due to its insensitivity to process light and incoherent plasma emissions.
A white light optical fiber interferometer is used to obtain the optical path length of an object and is then compared with the optical path length of a fixed reference arm. By using the spacing of the spectral interference fringes from the interferometer the optical path length can be calculated. The spectral interferogram intensity can approximately be described by

$$I(k) = A(k)\sum_{i=1}^{p}\left[\frac{I_{ref}}{2p} + \frac{I_i}{2} + \sqrt{I_{ref}I_i}\cos(2kz_i)\right]. \quad (1)$$

Equation (1) describes a set of p reflectors in the sample arm and z_i represents the optical path length difference from the reference length. *A(k)* is the spectral envelope of the imaging light for a wavenumber *k*. The first two terms can be ignored, the first is known and can be subtracted as background noise and the second is typically very small. In the third term the frequency of the sinusoidal interference fringe depends on its depth, z_i.

A depth-reflectivity profile of the sample, called A-line, is obtained by resampling the spectral interferogram to units of constant wavenumber by interpolation and transformed to *I(z)* via FFT. Each reflecting interface in the sample appears as a point spread function with its centre around the depth. The axial resolution of the system is defined by the full width at half maximum (FWHM) of the point spread function and for a Gaussian spectral envelope

$$\delta z = \frac{2\ln 2}{\pi}\frac{\lambda^2}{\Delta\lambda}. \quad (2)$$

Equation (2) shows that a short center wavelength λ and a broad spectrum Δλ) gives high axial resolution of the system. A higher axial resolution can be achieved by choosing a light source with broader spectrum but this will result in a reduced depth of view.

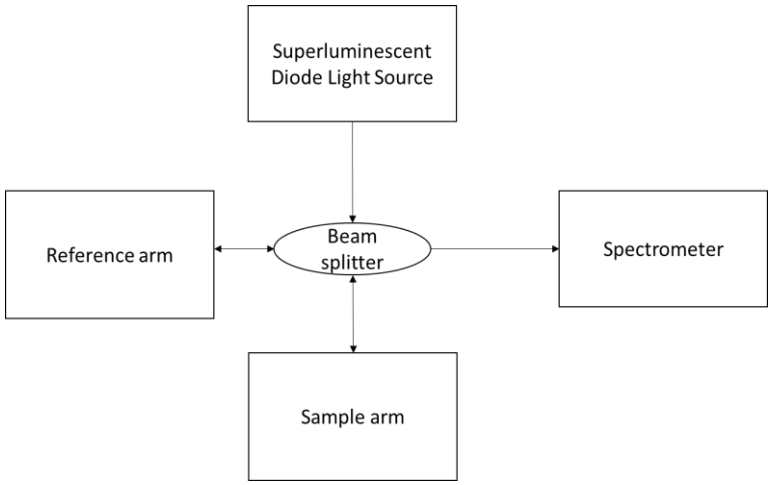

Fig. 4. Schematic block diagram of proposed system implementation.

The proposed system design by (Webster, Wright et al. 2011) consist of a superluminescent diode (SDL), a fiber optic Michelson interferometer and a custom made spectrometer. Coherent light from the SDL is split to the reference arm and the sample arm in the beam splitter. The retroreflected light from the reference arm and sample arm interfere in the beam splitter and is then passed to the spectrometer. In the spectrometer a camera measure the spectral interferogram and then transmits this data to a computer for processing. See Fig. 4 for a schematic picture.

2.5. Confocal methods

In confocal distance measurement, a point light source is imaged onto the measurement object. The same object point is further imaged onto a point sensor. If the object is in the focal distance, the image of the source on the object and the image of the object on the sensor is sharp and a high intensity is registered. If the object is out of the focal distance, both images are defocused and only a fraction of the light is registered by the sensor. Moving

the object or the focus in axial direction results in an intensity curve, which depends on the wavelength of light and the numerical aperture of the optical system (Wilson 1990).

A chromatic confocal point sensor achieves a complete parallelisation of the depth scan using chromatic aberration to achieve focal planes at different heights, each for one colour of the illumination light. The instrument uses a chromatic white-light sensor (CWL), which is based on the principle of chromatic aberration of light. White light is focused on the surface by a measuring head with a strongly wavelength-dependent focal length (chromatic aberration). The spectrum of the light scattered on the surface generates a peak in the spectrometer. The wavelength of this peak along with a calibration table reveals the distance from sensor to sample (Molesini, Pedrini et al. 1984; Dobson, Sun et al. 1997).

Some work is reported in literature (Wiesendanger, Körner et al. 2003; Wiesendanger, Körner et al. 2004) hinting that the method of confocal distance measurements has been used to estimate laser keyhole depth.

2.6. Laser Ultrasonic sensors

Laser ultrasonic is a non-contact measurement method that has the ability to measure thickness of material by using lasers for generation and detection of ultrasound (Lévesque, Kruger et al. 2006). Ultrasound is generated by a high power laser pulse causing a recoil effect on the surface which in turn produces longitudinal ultrasonic wave emission perpendicular to the surface like described in Fig. 5. These waves are reflected on the opposite side of the measurement object and then causes a small motion on the upper surface. A second laser is used to detect the ultrasonic signal of interest and an optical interferometer is used to demodulate scattered light that has been Doppler frequency shifted by the ultrasonic signal associated with the surface motion.

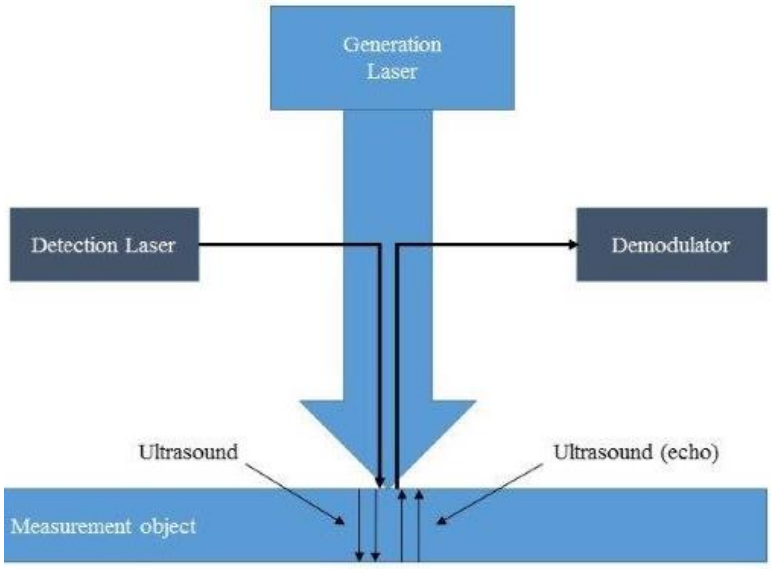

Fig. 5. Principle of laser ultrasonic sensor showing the generation laser, the detection laser and the perpendicular ultrasonic waves, outgoing and its echo, generated in the measurement object.

Thickness can be determined by measuring time of flight of the first ultrasonic echo reflected on the opposite side of the measurement object and a reference pulse.

3. TRANSMITTANCE MEASUREMENT OF THE LBW TOOL

Two different spectrometers were used to estimate the optical transmittance through the LBW tool as seen by the sensors since no such data was available to the authors. A CCD spectrometer, SPM002, from Photon Control Inc. was used to measure the transmittance in the wavelength range between 200-850nm. Another InGaAs spectrometer, BTC261-512-S, from B&W TEK Europe GmbH was used to measure the transmittance in the wavelength range between 900-1700nm. Both spectrometers are wavelength calibrated but not intensity calibrated. This implies that only relative transmittance can be estimated from the experiment. A tungsten halogen lamp was used as a reference source and the spectrometers was optically directed towards the reference and through the LBW optics. This reference source has practically no intensity at all in the ultra violet range

(100-400nm) resulting in a very uncertain estimate of the transmission in that particular range. The resulting normalised transmittance is shown in Fig. 6. It is clear that there is a significant transmittance in the regions between 400-600nm, 800-1000nm and 1200-1700nm. The transmittance stop bands are there to reflect the power laser beam (λ_{PLB}) and the low power pilot beam (λ_{pilot}) through the LBW tool focusing lens. Fig. 6 also shows the normalised black body radiation from a vapour plume at a temperature of 3000K. This point out that the presence of a dense vapour plume deteriorate the possibility to capture geometrical information from cameras with spectral sensitivity in the same range as the spectral information in the plume.

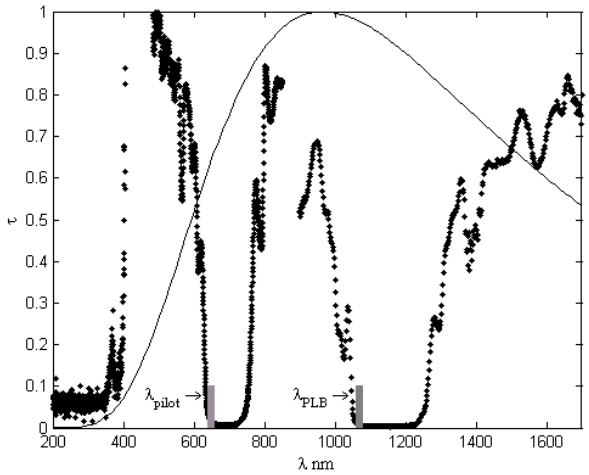

Fig. 6. Dotted line is LBW tool optical transmittance. Continous line is black-body radiation from vapour plume. Both curves are normalised to unity.

4. SUMMARY

The methods discussed and reported in this work are relevant for process monitoring of LBW and have been assessed by researchers with varying success. However, this literature survey reveals that there is an absence of thorough investigations of the robustness of the methods used in this context or an absence of discussions about the implications for industrial implementations. Table 2 gives a summary of the methods together with information of possible applications in LBW monitoring and sensor bandwidth. The summary is based on the findings in the references. The X-marks in this table indicates applicability in monitoring a certain weld defect. The question marks indicates that there is no reference confirming the assumption about the methods applicability but the authors believe that there is a reasonable possibility to use the method to monitor the weld defect. Finally the FP-mark indicates that this monitoring is only possible during full penetration welding. From Table 2 it is clear that the methods with a sampling rate of 1 kHz or below is best suited for pre- or post-monitoring e.g. gap detection misalignment, thickness, joint position and possible weld geometry to a certain extent. Methods with a sensor bandwidth well beyond 1 kHz could in turn be used for in-process monitoring of such features as focal point, weld depth, pores and spatter. This conclusion is also supported by the fact that the typical process time constants summarised in Table 1 is in the region of milliseconds.

Table 2. Summary of methods for laser welding monitoring.

Sensor	Sampling rate	Gap	Misalignment	Thickness	Joint position	Focal point	Weld depth	Pores	Spatter	Surface defect	Weld geometry
Visual camera	1 kHz	X			X	X	FP		X	X		
Camera + laser line	1 kHz	X	X		X	X	FP		X	X	X	
Laser ultrasound	100 Hz			X		X		X		X		
Infrared camera	1 kHz	X			X		FP		X	X		
Photo diode	150 kHz						FP		?			
Inline coheren imaging	30 kHz					X	X	?				
Confocal sensor	70 kHz					X	X					
Spektrometer	10 kHz						X	?	?			

REFERENCES

Bandoh, Y., Q. Guoping, et al. (2010). Recent advances in high dynamic range imaging technology. Image Processing (ICIP), 2010 17th IEEE International Conference on.

Beersiek, J. (2001). A CMOS camera as a tool for process analysis not only for laser beam welding. Proceedings of the International Congress of Applications of Lasers and Electro-Optics, Laser Institute of America.

Chen, G., M. Zhang, et al. (2013). "Measurements of laser-induced plasma temperature field in deep penetration laser welding." Optics & Laser Technology **45**(0): 551-557.

Dobson, S. L., P.-c. Sun, et al. (1997). "Diffractive lenses for chromatic confocal imaging." Applied Optics **36**(20): 4744-4748.

Fujinaga, S., H. Takenaka, et al. (2000). "Direct observation of keyhole behaviour during pulse modulated high-power Nd:YAG laser irradiation." Journal of Physics D: Applied Physics **33**(5): 492.

Greses, J., P. A. Hilton, et al. (2004). "Plume attenuation under high power Nd:yttritium–aluminum–garnet laser welding." Journal of Laser Applications **16**(1): 9-15.

Heralic, A., A.-K. Christiansson, et al. (2010). "Increased stability in laser metal wire deposition through feedback from optical measurements." Optics and Lasers in Engineering **48**(4): 478-485.

Huang, W. and R. Kovacevic (2011). "A Laser-Based Vision System for Weld Quality Inspection." Sensors **11**(1): 506-521.

Jager, M. and F. A. Hamprecht (2009). "Principal Component Imagery for the Quality Monitoring of Dynamic Laser Welding Processes." Industrial Electronics, IEEE Transactions on **56**(4): 1307-1313.

Kim, C.-H. and D.-C. Ahn (2012). "Coaxial monitoring of keyhole during Yb:YAG laser welding." Optics & Laser Technology **44**(6): 1874-1880.

Kong, F., J. Ma, et al. (2012). "Real-time monitoring of laser welding of galvanized high strength steel in lap joint configuration." Optics & Laser Technology **44**(7): 2186-2196.

Lévesque, D., S. E. Kruger, et al. (2006). "Thickness and grain size monitoring in seamless tube-making process using laser ultrasonics." NDT & E International **39**(8): 622-626.

M., D., P. M., et al. (2012). "Comprehensive Optical Monitoring of Selective Laser Melting." Journal of Laser Micro/Nanoengineering **7**(3): 236-243.

Molesini, G., G. Pedrini, et al. (1984). "Focus-wavelength encoded optical profilometer." Optics Communications **49**(4): 229-233.

Perret, O., M. Bizouard, et al. (2001). "Characterization of the keyhole formed during pulsed Nd–YAG laser interaction with a Ti–6Al–4V metallic target." Journal of Applied Physics **90**(1): 27-30.

Regaard, B., S. Kaierle, et al. (2009). "Seam-tracking for high precision laser welding applications—Methods, restrictions and enhanced concepts." Journal of Laser Applications **21**(4): 183-195.

Schmitt, R., G. Mallmann, et al. (2012). "Inline Process Metrology System for the Control of Laser Surface Structuring Processes." Physics Procedia **39**(0): 814-822.

Sibillano, T., D. Rizzi, et al. (2012). "Closed Loop Control of Penetration Depth during CO2 Laser Lap Welding Processes." Sensors **12**(8): 11077-11090.

Steen, W. M. and J. Mazumder (2010). Laser material processing. London, Springer.

Stritt, P., R. Weber, et al. (2011). "Utilizing Laser Power Modulation to Investigate the Transition from Heat-Conduction to Deep-Penetration Welding." Physics Procedia **12, Part A**(0): 224-231.

Webster, P. J. L., L. G. Wright, et al. (2011). "Automatic real-time guidance of laser machining with inline coherent imaging." Journal of Laser Applications **23**(2): -.

Wiesendanger, T., K. Körner, et al. (2004). Fast confocal point-sensor for in-process control of laser welding. ISMQ2004, 8th International Symposium on Measurement and Quality Control in Production, Erlangen, Germany.

Wiesendanger, T., K. Körner, et al. (2003). Fast confocal point-sensor for in-process control of laser welding. ICLAOM´03, International Conference on Laser Applications and Optical Metrology, New Delhi, India.

Wilson, T. (1990). Confocal microscopy, Academic Press.

Yousuke, K., O. Terumasa, et al. (2009). "In-process monitoring and feedback control for stable production of full-penetration weld in continuous wave fibre laser welding." Journal of Physics D: Applied Physics **42**(8): 085501.